

**A PARALLEL EIGENSOLVER USING CONTOUR INTEGRATION
FOR GENERALIZED EIGENVALUE PROBLEMS
IN MOLECULAR SIMULATION**

Tetsuya Sakurai*, Hiroto Tadano,
Tsutomu Ikegami and Umpei Nagashima

Abstract. In the present paper, we consider a parallel method for computing interior eigenvalues and corresponding eigenvectors of generalized eigenvalue problems arisen from molecular orbital computation in biochemistry applications. Matrices in such applications are sparse but often have a relatively large number of nonzero elements, and we may require some eigenpairs in a specific part of the spectrum. We use contour integration to construct a desired subspace. Properties of the subspace obtained by numerical integration are discussed, and a parallel implementation is then presented. We report the numerical aspects and parallel performance of the proposed method with matrices derived from molecular orbital computation.

1. INTRODUCTION

In the present paper, we consider a parallel method for computing eigenpairs (λ, \mathbf{x}) satisfying $A\mathbf{x} = \lambda B\mathbf{x}$ in a specific part of the spectrum arisen from molecular orbital computation, where $A, B \in \mathbb{R}^{n \times n}$ are symmetric and B is positive definite. Molecular orbital computation is performed in order to investigate phenomena such as the reaction mechanisms of enzymes and the electronic structure of photosynthetic systems.

The fragment molecular orbital (FMO) method [4] enables the total energy of a molecule to be calculated without performing molecular orbital computation for the entire molecule. In [1], a full electron calculation for a large molecule was performed using the FMO method on a massive cluster computer. The FMO-MO

Received September 1, 2008, accepted March 12, 2009.

2000 *Mathematics Subject Classification*: 65F15, 65E05, 65Y05.

Key words and phrases: Interior eigenvalue problems, Contour integration, Rayleigh-Ritz procedure, Biochemistry application.

*Corresponding author.

method [3, 12], which works as a post-process of the FMO method, gives a good approximation for canonical MOs without SCF iterations. A huge Fock matrix is generated, and we require a limited number of eigenpairs corresponding to frontier orbitals. Therefore, a large-scale interior eigenvalue problem occurs in the FMO-MO method.

With growing parallel efficiency in the Fock matrix construction, the diagonalization process becomes a bottleneck in MO calculations. Since the Fock matrix has a relatively large number of nonzero elements due to the base function of the middle-range interaction of molecules, a sparse factorization of the shifted matrix for spectral transformation may not be feasible. An alternative to factorization is offered by iterative solvers. Unfortunately, this is usually not an attractive option for parallel computation, because the iterative process is performed successively. Therefore, the shift-and-invert approach is not effective for treating interior eigenvalue problems in such applications.

The proposed method for finding eigenpairs in a given physical domain is based on the contour integral presented in [6]. One of the major advantages of the proposed eigensolver is that it does not require an inner loop to construct an approximate subspace or an outer loop to update approximate eigenvectors. Moreover, the values that are used in numerical integration can be evaluated independently on each integration node, which provides a variety of parallel programming models [7]. We recently proposed a Rayleigh-Ritz type method [8] in order to improve numerical stability. The block method [2] performs well if there are multiple eigenvalues in the interested spectrum.

The computation at each integral node involves linear system solutions in which the coefficient matrices are derived from A and B . In [5], we found that a Krylov subspace iterative method, in conjunction with a preconditioning using a complete factorization for an approximated coefficient matrix, is effective for solving such linear systems.

In the next section, we explain our eigensolver using contour integration. Then, we present some numerical properties of the subspace obtained by a numerical approximation of contour integration. In Section 3, we present an implementation of the proposed method. In Section 4, numerical examples are presented in order to verify the numerical properties and the parallel performance of the method with the matrices derived from molecular orbital computation.

2. AN EIGENSOLVER USING CONTOUR INTEGRATION

In this section, we describe an eigensolver using contour integration presented in [8]. This method finds eigenpairs inside a given circle. Let $(\lambda_i, \mathbf{x}_i)$, $1 \leq i \leq n$ be eigenpairs of the matrix pencil (A, B) . Suppose that m eigenvalues $\lambda_1, \dots, \lambda_m$

are located inside the circle Γ with center $\gamma \in \mathbb{R}$ and radius $\rho > 0$ in the complex plane. For a nonzero vector $\mathbf{v} \in \mathbb{R}^n$, let

$$(1) \quad \mathbf{s}_k = \frac{1}{2\pi i} \int_{\Gamma} z^k (zB - A)^{-1} B\mathbf{v} \, dz, \quad k = 0, 1, \dots, m-1,$$

and let $S = [\mathbf{s}_0, \dots, \mathbf{s}_{m-1}] \in \mathbb{R}^{n \times m}$.

Suppose that \mathbf{v} is expanded by the eigenvectors $\{\mathbf{x}_1, \dots, \mathbf{x}_n\}$ as

$$(2) \quad \mathbf{v} = \sum_{i=1}^n \alpha_i \mathbf{x}_i.$$

Then, we have the following theorem([8]).

Theorem 1. *If $\lambda_1, \dots, \lambda_m$ are distinct, and $\alpha_j \neq 0$ for $1 \leq j \leq m$, then*

$$\text{span}\{\mathbf{s}_0, \dots, \mathbf{s}_{m-1}\} = \text{span}\{\mathbf{x}_1, \dots, \mathbf{x}_m\}.$$

Let $Q = [\mathbf{q}_1, \dots, \mathbf{q}_m] \in \mathbb{R}^{n \times m}$ be an orthonormal matrix derived from $S = [\mathbf{s}_0, \dots, \mathbf{s}_{m-1}]$. Theorem 1 implies that the eigenpairs $(\lambda_i, \mathbf{x}_i)$, $1 \leq i \leq m$ can be extracted using the Rayleigh-Ritz procedure with the projected matrix pencil $(Q^T A Q, Q^T B Q)$.

We approximate the contour integral (1) via the N -point trapezoidal rule:

$$\hat{\mathbf{s}}_k = \frac{1}{N} \sum_{j=0}^{N-1} \left(\frac{\omega_j - \gamma}{\rho} \right)^{k+1} (\omega_j B - A)^{-1} B\mathbf{v}, \quad k = 0, 1, \dots, m-1$$

where $\omega_j = \gamma + \rho \exp(2\pi i(j + 1/2)/N)$ and N is a positive integer.

In this computation, we solve the following systems of linear equations

$$(3) \quad (\omega_j B - A)\mathbf{y}_j = B\mathbf{v}, \quad j = 0, 1, \dots, N-1$$

for $\mathbf{y}_0, \dots, \mathbf{y}_{N-1} \in \mathbb{C}^n$. The solutions $\mathbf{y}_{N/2}, \dots, \mathbf{y}_{N-1}$ are obtained from the relation $\mathbf{y}_j = \bar{\mathbf{y}}_{N-j-1}$. Thus, we only need to solve $N/2$ systems, and

$$(4) \quad \hat{\mathbf{s}}_k = \frac{1}{N} \sum_{j=0}^{N/2-1} 2 \operatorname{Re} \left(\left(\frac{\omega_j - \gamma}{\rho} \right)^{k+1} \mathbf{y}_j \right), \quad k = 0, 1, \dots, m-1.$$

Note that $\hat{\mathbf{s}}_k$ are real vectors.

Letting $\theta_j = \exp(2\pi i(j + 1/2)/N)$, the following relations hold:

Lemma 2. Let η be a real number with $|\eta| \neq 1$. For an integer k ($1 \leq k < N$), the following holds:

$$(5) \quad \frac{1}{N} \sum_{j=0}^{N-1} \frac{\theta_j^{k+1}}{\theta_j - \eta} = \frac{\eta^k}{1 + \eta^N}.$$

Proof. If $|\eta| < 1$, we have

$$(6) \quad \begin{aligned} \frac{1}{N} \sum_{j=0}^{N-1} \frac{\theta_j^{k+1}}{\theta_j - \eta} &= \frac{1}{N} \sum_{j=0}^{N-1} \frac{\theta_j^k}{1 - \frac{\eta}{\theta_j}} \\ &= \sum_{p=0}^{\infty} \eta^p \frac{1}{N} \sum_{j=0}^{N-1} \theta_j^{k-p} \\ &= \sum_{q=0}^{\infty} (-1)^q \eta^{Nq+k}. \end{aligned}$$

The last step follows from the fact that

$$(7) \quad \frac{1}{N} \sum_{j=0}^{N-1} \theta_j^p = \begin{cases} (-1)^q & \text{if } p = qN \text{ for } q \in \mathbb{Z} \\ 0 & \text{otherwise} \end{cases}.$$

Similarly, for the case in which $|\eta| > 1$, we have

$$(8) \quad \begin{aligned} \frac{1}{N} \sum_{j=0}^{N-1} \frac{\theta_j^{k+1}}{\theta_j - \eta} &= \frac{1}{N} \sum_{j=0}^{N-1} \left(\frac{-1}{\eta} \right) \frac{\theta_j^{k+1}}{1 - \frac{\theta_j}{\eta}} \\ &= \sum_{p=0}^{\infty} \left(\frac{-1}{\eta^{p+1}} \right) \left(\frac{1}{N} \sum_{j=0}^{N-1} \theta_j^{p+k+1} \right) \\ &= \sum_{q=1}^{\infty} (-1)^{q-1} \eta^{-Nq+k}. \end{aligned}$$

Thus, (5) is obtained from (6) and (8). ■

Theorem 3. Let $\eta_i = (\lambda_i - \gamma)/\rho$, $1 \leq i \leq n$, then

$$(9) \quad \hat{\mathbf{s}}_k = \sum_{i=1}^n \frac{\alpha_i}{\rho} \cdot \frac{\eta_i^k}{1 + \eta_i^N} \mathbf{x}_i.$$

Proof. Since

$$(\omega_j B - A)^{-1} B \mathbf{x}_i = \frac{1}{\omega_j - \lambda_i} \mathbf{x}_i,$$

it follows that

$$\begin{aligned}
 \hat{\mathbf{s}}_k &= \frac{1}{N} \sum_{j=0}^{N-1} \left(\frac{\omega_j - \gamma}{\rho} \right)^{k+1} (\omega_j B - A)^{-1} B \mathbf{v} \\
 &= \frac{1}{N} \sum_{j=0}^{N-1} \left(\frac{\omega_j - \gamma}{\rho} \right)^{k+1} \sum_{i=1}^n \alpha_i (\omega_j B - A)^{-1} B \mathbf{x}_i \\
 &= \frac{1}{N} \sum_{j=0}^{N-1} \left(\frac{\omega_j - \gamma}{\rho} \right)^{k+1} \sum_{i=1}^n \frac{\alpha_i}{\omega_j - \lambda_i} \mathbf{x}_i \\
 &= \sum_{i=1}^n \frac{\alpha_i}{\rho} \left(\frac{1}{N} \sum_{j=0}^{N-1} \frac{\theta_j^{k+1}}{\theta_j - \eta_i} \right) \mathbf{x}_i.
 \end{aligned}$$

Therefore, from Lemma 2, we have

$$\hat{\mathbf{s}}_k = \sum_{i=1}^n \frac{\alpha_i}{\rho} \cdot \frac{\eta_i^k}{1 + \eta_i^N} \mathbf{x}_i.$$

This proves the theorem. ■

For vectors $\mathbf{a}, \mathbf{b} \in \mathbb{R}^n$, we define the B inner product $\langle \cdot, \cdot \rangle_B$ by

$$\langle \mathbf{a}, \mathbf{b} \rangle_B = \mathbf{a}^T B \mathbf{b}.$$

From Theorem 3, we have the following estimation for eigencomponents that are included in $\hat{\mathbf{s}}_k$.

Theorem 4. *Assume that the eigenvectors $\mathbf{x}_1, \dots, \mathbf{x}_n$ are normalized to be B -orthogonal, i.e., $\langle \mathbf{x}_i, \mathbf{x}_j \rangle_B = \delta_{ij}$. Then,*

$$|\langle \mathbf{x}_i, \hat{\mathbf{s}}_k \rangle_B| = \begin{cases} \frac{\alpha_i}{\rho} \eta_i^k + O(|\eta_i|^{N+k}) & (1 \leq i \leq m) \\ O(|\eta_i|^{-N+k}) & (m+1 \leq i \leq n) \end{cases}.$$

From this theorem, we can see that the eigencomponent in $\hat{\mathbf{s}}_k$ with respect to λ_i decays exponentially with the ratio $|\eta_i| = |\lambda_i - \gamma|/\rho$, if λ_i is located outside Γ .

A block variant of the eigensolver is proposed in [2], which enables us to obtain degenerate eigenvalues. In the eigensolver, a matrix $V = [\mathbf{v}_1, \dots, \mathbf{v}_L] \in \mathbb{R}^{n \times L}$ is used instead of \mathbf{v} in (3), where $\mathbf{v}_1, \dots, \mathbf{v}_L$ are linearly independent, and positive integer L is the block size. Then, the numerical integration in (4) is represented as

$$\hat{S}_k = \frac{1}{N} \sum_{j=0}^{N/2-1} 2 \operatorname{Re} \left(\left(\frac{\omega_j - \gamma}{\rho} \right)^{k+1} Y_j \right) \quad k = 0, 1, \dots, M-1,$$

with the following systems of linear equations

$$(10) \quad (\omega_j B - A)Y_j = BV, \quad j = 0, 1, \dots, N/2 - 1,$$

where M is a positive integer chosen so that $M \geq m/L$.

In choosing the size of the subspace, we use the singular value of $\hat{S} = [\hat{S}_0, \dots, \hat{S}_{M-1}]$. Let $U^T \Sigma W = \hat{S}$ be a singular value decomposition of \hat{S} , and let $\Sigma = \text{diag}(\sigma_1, \dots, \sigma_M)$. Let \hat{m} be an integer such that $\sigma_j/\sigma_1 \geq \delta$ for $1 \leq j \leq \hat{m}$ and $\sigma_j/\sigma_1 < \delta$ for $j > \hat{m}$. Then, the orthonormal matrix $\tilde{Q} \in \mathbb{R}^{n \times \hat{m}}$ is constructed from $\hat{S}(:, 1 : \hat{m})$. The algorithm is shown below.

Algorithm (block method using contour integration):

Input $A, B \in \mathbb{R}^{n \times n}$, $V \in \mathbb{R}^{n \times L}$, N, M, δ

Output $(\hat{\lambda}_i, \hat{x}_i)$, $1 \leq i \leq \hat{m}$

1. Solve $(\omega_j B - A)Y_j = BV$ for Y_j , $j = 0, \dots, N/2 - 1$
2. Compute $\hat{S}_k = \sum_{j=0}^{N/2-1} 2\text{Re}(\theta_j^{k+1} Y_j)$, $k = 0, \dots, M - 1$
3. Perform singular value decomposition $U^T \Sigma W = [\hat{S}_0, \dots, \hat{S}_{M-1}]$, and find \hat{m} such that $|\sigma_j|/|\sigma_1| \geq \delta$ for $1 \leq j \leq \hat{m}$
4. Construct an orthonormal basis \tilde{Q} from $\hat{S}(:, 1 : \hat{m})$
5. Form $\tilde{A} = \tilde{Q}^T A \tilde{Q}$ and $\tilde{B} = \tilde{Q}^T B \tilde{Q}$
6. Compute the eigenpairs $(\hat{\lambda}_l, \hat{w}_l)$, $1 \leq l \leq \hat{m}$ of the projected pencil (\tilde{A}, \tilde{B})
7. Set $\hat{x}_i = \tilde{Q} \hat{w}_i$, $1 \leq l \leq \hat{m}$

Note that we can use $U(:, 1 : \hat{m})$ instead of \tilde{Q} so as to avoid the orthogonalization of $\hat{S}(:, 1 : \hat{m})$.

3. AN IMPLEMENTATION

When matrices A and B are large, the computational costs for solving systems of linear equations (10) are dominant. In the present implementation, the matrices have a relatively large number of nonzero elements, which could make sparse direct methods impractical due to the large number of fill-ins required. Instead, we apply a Krylov subspace iterative method with the complete factorization preconditioner presented in [5].

In the preconditioning method of the present study, a complete factorization of the approximate matrix $\tilde{C}_j = (\tilde{c}_{ij})$ of the coefficient matrix $C_j := \omega_j B - A$ is performed. The approximate matrix \tilde{C}_j is obtained from the drop-thresholding of

the original coefficient matrix C_j . Since there are fewer nonzero elements in \tilde{C}_j than in C_j , we expect fewer nonzero elements in the preconditioner than the matrix factor obtained from complete factorization of C_j . Drop-thresholding is defined as follows:

$$\tilde{c}_{ij} = \begin{cases} c_{ij} & (|c_{ij}| > \varepsilon) \\ 0 & (|c_{ij}| \leq \varepsilon) \end{cases},$$

where ε is a small positive number.

Since systems (10) can be solved independently for j , we solve $N/2$ systems

$$(11) \quad C_j Y_j = BV, \quad j = 0, 1, \dots, N/2 - 1$$

on each computing node of clusters. Before starting the iterative process of the Krylov subspace method, the approximate matrix \tilde{C}_j is factorized, and then forward/backward substitutions and matrix-vector multiplications are performed in the iterative process.

We can easily extend the method for the case in which several circular regions are given. Suppose that N_c circles $\Gamma^{(0)}, \dots, \Gamma^{(N_c-1)}$ with center $(\gamma^{(l)}, \rho^{(l)})$ and radius $0 \leq l \leq N_c - 1$ are given. Then, we solve $N_c \times (N/2)$ linear systems

$$(\omega_j^{(l)} B - A) Y_j^{(l)} = BV, \quad j = 0, \dots, N/2 - 1, \quad l = 0, \dots, N_c - 1,$$

where $\omega_j^{(l)} = \gamma^{(l)} + \rho^{(l)} \exp(2\pi i(j+1/2)/N)$, $j = 0, \dots, N/2 - 1$ are equidistributed points on the l -th circle $\Gamma^{(l)}$. We solve these linear systems simultaneously on distributed computing nodes.

First, we broadcast the sparse matrix data of A and B to all computing nodes. Then, we start to solve systems of linear equations on the computing nodes simultaneously. After that, we construct a subspace for each circle using the results of the linear solver, and then perform the Rayleigh-Ritz procedure to extract eigenpairs in each circle. Since the computational costs to solve systems of linear equations dominate the computations, we can expect high performance in parallel computations. The algorithm for parallel implementation is summarized as follows:

Parallel implementation (circles $\Gamma_0, \dots, \Gamma_{N_c-1}$):

1. Broadcast sparse matrix data of A and B
2. do $l = 0, 1, \dots, N_c - 1$
3. Solve $(\omega_j^{(l)} B - A) Y_j^{(l)} = BV$ for $Y_j^{(l)}$, $j = 0, \dots, N/2 - 1$
4. AllReduce $2\text{Re}(\theta_j^{(l)})^{k+1} Y_j^{(l)}$, $j = 0, \dots, N/2 - 1$, and compute $\hat{S}_k^{(l)} = \sum_{j=0}^{N/2-1} 2\text{Re}((\theta_j^{(l)})^{k+1} Y_j^{(l)})$, $k = 0, \dots, M - 1$
5. Compute singular values $\sigma_1^{(l)}, \dots, \sigma_M^{(l)}$ of $\hat{S}^{(l)} = [\hat{S}_0^{(l)}, \dots, \hat{S}_{M-1}^{(l)}]$,

- and set $\hat{m}^{(l)}$ such that $|\sigma_j^{(l)}|/|\sigma_1^{(l)}| \geq \delta$ for $1 \leq j \leq \hat{m}^{(l)}$
6. Construct the orthonormal basis $\tilde{Q}^{(l)}$ from $\hat{S}^{(l)}(:, 1 : \hat{m}^{(l)})$
 7. Form $\tilde{A}^{(l)} = (\tilde{Q}^{(l)})^T A \tilde{Q}^{(l)}$ and $\tilde{B}^{(l)} = (\tilde{Q}^{(l)})^T B \tilde{Q}^{(l)}$
 8. Compute the eigenpairs $(\hat{\lambda}_i^{(l)}, \hat{w}_i^{(l)})$, $1 \leq i \leq \hat{m}^{(l)}$ of the projected pencil $(\tilde{A}^{(l)}, \tilde{B}^{(l)})$
 9. Set $\hat{x}_i^{(l)} = \tilde{Q}^{(l)} \hat{w}_i^{(l)}$, $1 \leq i \leq \hat{m}^{(l)}$
 10. end do

4. NUMERICAL EXAMPLES

In this section, we present numerical examples with the matrices derived from the FMO-MO method[10].

Example 1. The test matrices A and B are derived from the computation of the molecular orbitals of an eight-base-pair model DNA. The size of the matrices is $n = 1,980$, and the number of nonzero elements is 728,080.

The CPU was a Core2Duo (2.2 GHz) with 2 GB of memory. Computation was performed using MATLAB 7.5 with double-precision arithmetic. The systems of linear equations were solved by the sparse direct solver UMFPACK in MATLAB. The elements of V were distributed randomly on the interval $[0, 1]$ by a random number generator. The exact eigenpairs (λ_i, x_i) $1 \leq i \leq n$ were evaluated by the MATLAB command `eig`.

In Figure 1, we show $|\langle x_i, \hat{s}_0 \rangle_B|$ with respect to eigenvalues $\lambda_i \in [-0.25, -0.16]$. The parameters were $\gamma = -0.2$, $\rho = 0.01$, $N = 32$, $L = 12$, $M = 12$, and $\delta = 10^{-12}$. In this case, the interval $[-0.21, -0.19]$ is inside and on Γ . The eigencomponents associated with eigenvalues that are located outside Γ decay exponentially to zero in \hat{s}_0 . For vectors \hat{s}_k , $k \geq 1$, we can obtain similar results. In Figure 2, we show $|\langle \hat{x}_i, \tilde{Q} \rangle_B|$. We can see that \tilde{Q} includes only the eigencomponents around the interval $[-0.21, -0.19]$.

In Table 1, the error and residual of approximate eigenvalues in Γ are shown. A total of 16 eigenvalues are located in the interval $[-0.21, -0.19]$, and all of the eigenvalues in this interval were obtained with sufficient accuracy.

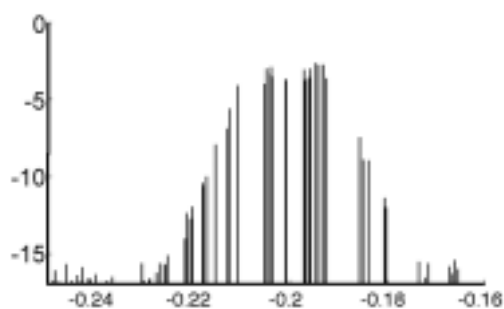


Fig. 1. $|\langle \mathbf{x}_i, \hat{\mathbf{s}}_0 \rangle_B|$ ($\gamma = -0.2$, $\rho = 0.01$, $N = 32$).

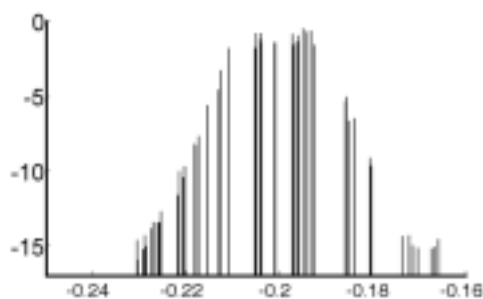


Fig. 2. $|\langle \tilde{\mathbf{x}}_i, \tilde{\mathbf{Q}} \rangle_B|$ ($\gamma = -0.2$, $\rho = 0.01$, $N = 32$).

Example 2. The test matrices were obtained from an epidermal growth factor receptor (EGFR) protein, which is a target molecule for anticancer agents. The Fock matrix was constructed by the method described in [10]. The dimension of the Fock matrix was 96,234, and the number of non-zero elements was 457 million.

The calculations were performed on a P32 subsystem of the AIST Super Cluster (ASC) at National Institute of Advanced Industrial Science and Technology Agency (AIST). Each computing node is an Opteron Dual processor (2.0 GHz) with 6 GB of memory and is interconnected by both Myrinet and gigabit ethernet. Intel C and Fortran compiler 9.1 were used to compile the codes with Intel Math Kernel Library 10.0.

The number of integration points was $N = 32$, and the block size was $L = 16$. We placed eight circles around the highest occupied molecular orbital (HOMO) and the lowest unoccupied molecular orbital (LUMO) using the approximate eigenvalues obtained from the results of the FMO method. The total number of systems to be solved was $8 \times (32/2) = 128$ with 16 right-hand-side vectors. Since each system of linear equations was solved on a single node of a dual processor, 16 nodes (32 PUs) were used for one circle. Thus, a total of 256 PUs were used.

Table 1: Errors and residuals in Example 1

i	$\hat{\lambda}_i$	$ \hat{\lambda}_i - \lambda_i $	$\ A\hat{x}_i - \hat{\lambda}_i B\hat{x}_i\ _2$
1	-0.192423480937650	2.9×10^{-15}	9.4×10^{-15}
2	-0.193053272393176	3.7×10^{-15}	1.6×10^{-14}
3	-0.193867518039814	1.1×10^{-15}	1.0×10^{-14}
4	-0.194749418147652	2.0×10^{-14}	2.0×10^{-14}
5	-0.195768218806505	2.5×10^{-15}	2.5×10^{-14}
6	-0.196048479728466	7.2×10^{-16}	2.8×10^{-14}
7	-0.196721896535061	1.2×10^{-15}	4.0×10^{-14}
8	-0.197042777317239	4.7×10^{-16}	5.5×10^{-14}
9	-0.200591957877910	1.2×10^{-15}	5.5×10^{-13}
10	-0.200835717839500	5.8×10^{-16}	1.9×10^{-13}
11	-0.203655629362533	2.5×10^{-16}	5.6×10^{-14}
12	-0.203800310807316	1.4×10^{-16}	4.4×10^{-14}
13	-0.203932047603002	6.1×10^{-16}	4.4×10^{-14}
14	-0.204805988179016	3.4×10^{-15}	1.6×10^{-14}
15	-0.204824251443765	2.6×10^{-15}	3.4×10^{-14}
16	-0.205054724756940	1.3×10^{-14}	2.8×10^{-14}

The preconditioned COCG method[11] was used as the iterative linear solver. The stopping criterion for the relative residual norm was 10^{-10} . The preconditioner was constructed by applying a complete factorization for an approximate coefficient matrix, which was obtained from drop-thresholding of the original coefficient matrix. The drop-thresholding parameter was 2×10^{-4} . The complete factorization is performed by a sparse direct solver in the PARDISO library [9]. The elements of V were distributed randomly on the interval $[0, 1]$ by a random number generator.

The timing results are shown in Figure 3. The wall-clock time was 602 seconds, and 94 eigenpairs were obtained. The time to broadcast the matrix data to all computing nodes was 36.4 seconds, and the time to solve linear systems was 563.8 seconds. The maximum residual of these eigenpairs was 3.4×10^{-10} .

Figure 4 shows the amount of time of each step in the algorithm for the circle $\Gamma^{(7)}$, where gray, light gray, white, and black segments represent the factorization times for the approximate matrix, forward and backward substitution in iteration, matrix-vector multiplication, and the Rayleigh-Ritz procedure, respectively.

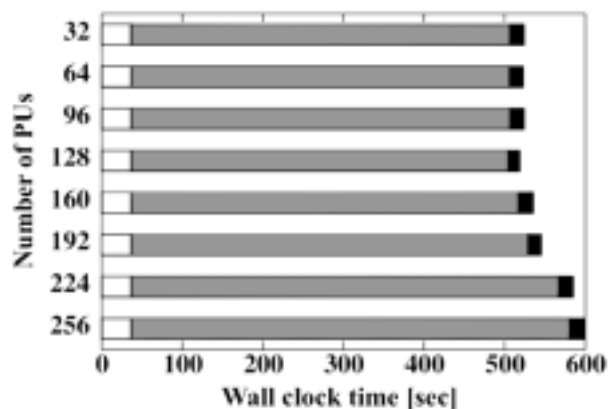


Fig. 3. Timing results of the method with 256 PUs in seconds. Each bar represents the wall-clock time for one circle. For each circle, 32 PUs were used, for a total of 256 PUs. [□]: Broadcast (white), [■]: Linear system solver (Gray), [■]: Rayleigh-Ritz procedure (black)].

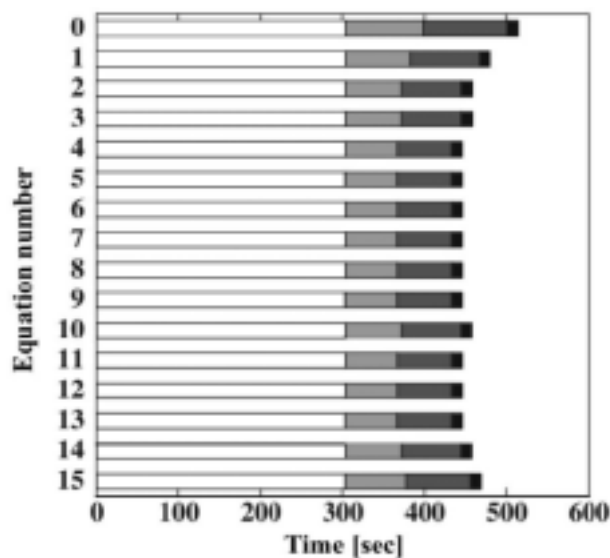


Fig. 4. Time for each process for one circle. Each bar represents the time on one integration node. A total of 16 systems of linear equations were solved. [□]: Factorization (white), [■]: Forward/backward Substitution (gray), [■]: Matrix-vector multiply (deep gray), [■]: Rayleigh-Ritz procedure (black)].

5. CONCLUSIONS

A parallel method for computing interior eigenvalues and corresponding eigenvectors of generalized eigenvalue problems that arise from molecular orbital com-

putation was considered. In the present application, matrices often have a relatively large number of nonzero elements, and eigenpairs are required in a specific part of the spectrum.

We applied a Rayleigh-Ritz procedure with numerical integration. In this method, contour integration is used to construct a desired subspace. The proposed eigensolver does not require inner and outer loops to construct an approximate subspace and update approximate eigenvectors. For the computation of the contour integrals, we solve a number of systems of linear equations. When A and B are large, the computational costs for solving these systems of linear equations are dominant. Since these linear systems can be solved independently for each integration node, the process by which to derive the subspace is performed in parallel.

We showed that the subspace obtained by numerical integration includes eigenvectors corresponding to the eigenvalues around the interested interval. The i -th eigencomponent in the subspace decays exponentially to zero with a rate $|\lambda_i - \gamma|/\rho$, if the corresponding eigenvalue λ_i is located outside the interval.

The numerical experiments indicate that the proposed method gives good parallel performance and that desired eigenpairs can be obtained with sufficient accuracy. In the future, we intend to estimate appropriate parameters with theoretical analysis and compare the proposed method with other methods.

ACKNOWLEDGMENT

The present study was supported in part by CREST of the Japan Science and Technology Agency (JST).

REFERENCES

1. T. Ikegami, T. Ishida, D. G. Fedorov, K. Kitaura, Y. Inadomi, H. Umeda, M. Yokokawa and S. Sekiguchi, *Full electron calculation beyond 20,000 atoms: ground electronic state of photosynthetic proteins*, Proceedings of Supercomputing 2005, Seattle, Washington, USA. 2005.
2. T. Ikegami, T. Sakurai and U. Nagashima, A filter diagonalization for generalized eigenvalue problems based on the Sakurai-Sugiura projection method, *J. Comput. Appl. Math.*, **233** (2010), 1927-1936.
3. Y. Inadomi, T. Nakano, K. Kitaura and U. Nagashima, Definition of molecular orbitals in fragment molecular orbital method, *Chem. Phys. Lett.*, **364** (2002), 139-143.
4. K. Kitaura, T. Sawai, T. Asada, T. Nakano and M. Uebayasi, Pair interaction molecular orbital method: an approximate computational method for molecular interactions. *Chem. Phys. Lett.*, **312** (1999), 319-324.
5. M. Okada, T. Sakurai and K. Teranishi, *A preconditioner for krylov subspace method using a sparse direct solver. Abstract of Precond'07*, Toulouse, 2007.

6. T. Sakurai and H. Sugiura, A projection method for generalized eigenvalue problems, *J. Comput. Appl. Math.*, **159** (2003), 119-128.
7. T. Sakurai, Y. Kodaki, H. Tadano, H. Umeda, Y. Inadomi, T. Watanabe and U. Nagashima, *A master-worker type eigensolver for molecular orbital computations*, Kagstrom, B., Elmroth, E., Dongarra, Wasniewski, J. (eds.), PARA'06. LNCS No. 4699, 617-625, Springer, Heidelberg 2007.
8. T. Sakurai and T. Tadano, CIRR: a Rayleigh-Ritz type method with contour integral for generalized eigenvalue problems, In: The First China-Japan-Korea Joint Conference on Numerical Mathematics, *Special Issue of Hokkaido Math. J.*, **36** (2007), 745-757.
9. O. Schenk and K. Gärtner, Solving unsymmetric sparse systems of linear equations with PARDISO, *Future Generation Comput. Sys.*, **20** (2004), 475-487.
10. H. Umeda, Y. Inadomi, T. Watanabe, T. Ishimoto and U. Nagashima, *Grid-enabled parallel Fock matrix construction*, *Abstract of MATH/CHEM/COMP 2007 (MCC'07)*, Dubrovnik, Croatia, 2007.
11. H. A. van der Vorst and J. B. M. Melissen, A Petrov-Galerkin type method for solving $Ax = b$, where A is a symmetric complex matrix, *IEEE Trans. on Magnetism*, **26** (1990), 706-708.
12. T. Watanabe, Y. Inadomi, T. Ishimoto, H. Umeda, T. Sakurai and U. Nagashima, Molecular orbital calculation for large molecule, *J. Comput. Chem. Japan*, **6** (2007), 217-226.

Tetsuya Sakurai and Hiroto Tadano
Department of Computer Science,
University of Tsukuba,
1-1-1 Tennodai,
Tsukuba, Ibaraki 305-8573,
Japan
E-mail: sakurai@cs.tsukuba.ac.jp

Tsutomu Ikegami and Umpei Nagashima
National Institute of Advanced Industrial Science and Technology,
1-1-1 Umezono,
Tsukuba, Ibaraki 305-8568,
Japan